

# Critical behavior at Mott-Anderson transition: a TMT-DMFT perspective

M. C. O. Aguiar,<sup>1</sup> V. Dobrosavljević,<sup>2</sup> E. Abrahams,<sup>3</sup> and G. Kotliar<sup>3</sup>

<sup>1</sup>*Departamento de Física, Universidade Federal de Minas Gerais,  
Av. Antônio Carlos, 6627, Belo Horizonte, MG, Brazil*

<sup>2</sup>*Department of Physics and National High Magnetic Field Laboratory,  
Florida State University, Tallahassee, FL 32306, USA*

<sup>3</sup>*Center for Materials Theory, Serin Physics Laboratory, Rutgers University,  
136 Frelinghuysen Road, Piscataway, New Jersey 08854, USA*

We present a detailed analysis of the critical behavior close to the Mott-Anderson transition. Our findings are based on a combination of numerical and analytical results obtained within the framework of Typical-Medium Theory (TMT-DMFT) - the simplest extension of dynamical mean field theory (DMFT) capable of incorporating Anderson localization effects. By making use of previous scaling studies of Anderson impurity models close to the metal-insulator transition, we solve this problem analytically and reveal the dependence of the critical behavior on the particle-hole symmetry. Our main result is that, for sufficiently strong disorder, the Mott-Anderson transition is characterized by a precisely defined two-fluid behavior, in which only a fraction of the electrons undergo a “site selective” Mott localization; the rest become Anderson-localized quasiparticles.

PACS numbers: 71.27.+a, 72.15.Rn, 71.30.+h

Many strongly correlated materials find themselves close to Mott localization [1] - a process through which all the valence electrons within a narrow band turn into localized magnetic moments. In real systems, disorder introduced by doping or impurities often cannot be neglected, as it provides an alternative fundamental mechanism for suppressing metallicity, through the process of Anderson localization [2]. The effects of weak interactions in this regime have been studied using perturbative methods [3], but these approaches cannot describe the strong correlation effects associated with incipient magnetism and Mott localization.

Which of these two routes to localization - Anderson or Mott - dominate? In most cases, simple estimates show that both effects play a comparable role and both need to be taken into account. Most existing theories are not able to combine these two fundamental processes in the same framework, and this conceptual difficulty has provided the essential pitfall in our understanding of the metal-insulator transition (MIT).

At the moment, the most successful theory for the Mott transition is based on dynamical mean field theory (DMFT) [4] ideas. By replacing the environment of each site by its average value, the original version of this theory proved unable to describe the spatial fluctuation effects associated with the approach to the Anderson transition. Very recent work [5], however, identified the conceptually simplest extension of DMFT capable to overcome these shortcomings - the Typical-Medium Theory (TMT-DMFT). In the non-interacting limit, this theory provides a reasonable picture of the Anderson transition, as established by quantitative comparison [5] with exact (numerical) results.

The TMT-DMFT method was first applied to the disordered Hubbard model by Byczuk *et al.* [6], who ob-

tained the phase diagram for this problem from the numerical solution using the Numerical Renormalization Group (NRG) method for the impurity solver. However, the physical nature of the phases and of the phase transition was not investigated in that numerical study.

The task of elucidating the physical mechanism and the precise form of the Mott-Anderson critical point within the TMT-DMFT description is the main subject of this Letter. By making use of previous scaling studies [7] of Anderson impurity models close to the MIT, we present a detailed analytic solution for this problem, which emphasizes the dependence of the system properties on its particle-hole symmetry. Our main finding is that, for sufficiently strong disorder, the physical mechanism behind the Mott-Anderson transition is the formation of two fluids, a behavior that is surprisingly reminiscent of the phenomenology proposed for doped semiconductors [8]. Here, only a fraction of the electrons (sites) undergo Mott localization; the rest can be described as Anderson-localized quasiparticles. Thus, in our picture the Mott-Anderson transition can be seen as reminiscent of the “orbitally selective” Mott localization [9]; precisely, here we have a “site selective” Mott transition, since it emerges in a spatially resolved fashion.

*TMT-DMFT and order parameters* - We consider a half-filled Hubbard model [4] with random site energies, as given by the Hamiltonian

$$H = -V \sum_{\langle ij \rangle \sigma} c_{i\sigma}^\dagger c_{j\sigma} + \sum_{i\sigma} \varepsilon_i n_{i\sigma} + U \sum_i n_{i\uparrow} n_{i\downarrow}. \quad (1)$$

Here,  $c_{i\sigma}^\dagger$  ( $c_{i\sigma}$ ) creates (destroys) a conduction electron with spin  $\sigma$  on site  $i$ ,  $n_{i\sigma} = c_{i\sigma}^\dagger c_{i\sigma}$ ,  $V$  is the hopping amplitude, and  $U$  is the on-site repulsion. The random on-site energies  $\varepsilon_i$  follow a distribution  $P(\varepsilon)$ , which is assumed to be uniform and have width  $W$ .

TMT-DMFT [5, 6] maps the lattice problem onto an ensemble of single-impurity problems, corresponding to sites with different values of the local energy  $\varepsilon_i$ , each being embedded in a typical effective medium which is self-consistently calculated. In contrast to standard DMFT [10], TMT-DMFT determines this effective medium by replacing the spectrum of the environment (“cavity”) for each site by its typical value, which is determined by the process of *geometric* averaging. For a simple semi-circular model density of states, the corresponding bath function is given by [5, 6]  $\Delta(\omega) = V^2 G_{typ}(\omega)$ , with  $G_{typ}(\omega) = \int_{-\infty}^{\infty} d\omega' \rho_{typ}(\omega') / (\omega - \omega')$  being the Hilbert transform of the geometrically-averaged (typical) local density of states (LDOS)  $\rho_{typ}(\omega) = \exp\{\int d\varepsilon P(\varepsilon) \ln \rho(\omega, \varepsilon)\}$ . Given the bath function  $\Delta(\omega)$ , one first needs to solve the local impurity models and compute the local spectra  $\rho(\omega, \varepsilon) = -\pi^{-1} \text{Im} G(\omega, \varepsilon)$ , and the self-consistency loop is then closed by the the geometric averaging procedure.

To qualitatively understand the nature of the critical behavior, it is useful to concentrate on the low-energy form for the local Green’s functions, which can be specified in terms of two Fermi liquid parameters as

$$G(\omega, \varepsilon_i) = \frac{Z_i}{\omega - \tilde{\varepsilon}_i - Z_i \Delta(\omega)}, \quad (2)$$

where  $Z_i$  is the local quasi-particle (QP) weight and  $\tilde{\varepsilon}_i$  is the renormalized site energy [10]. The parameters  $Z_i$  and  $\tilde{\varepsilon}_i$  can be obtained using any quantum impurity solver, but to gain analytical insight here we focus on the variational calculation provided by the “four-boson” technique (SB4) of Kotliar and Ruckenstein [11], which is known to be quantitatively accurate at  $T = 0$ . We should stress, though, that most of our analytical results rely only on Fermi liquid theorems constraining the qualitative behavior at low energy, and thus do not suffer from possible limitations of the SB4 method.

Within this formulation, the metal is identified by nonzero QP weights  $Z_i$  on *all* sites and, in addition, a nonzero value for both the typical and the average  $[\rho_{av}(\omega) = \int d\varepsilon P(\varepsilon) \rho(\omega, \varepsilon)]$  LDOS. Mott localization (i.e. local moment formation) is signaled by  $Z_i \rightarrow 0$  [10], while Anderson localization corresponds to  $Z_i \neq 0$  and  $\rho_{av} \neq 0$ , but  $\rho_{typ} = 0$  [2, 5]. While Ref. [6] concentrated on  $\rho_{typ}$  and  $\rho_{av}$ , we find it useful to simultaneously examine the QP weights  $Z_i$ , in order to provide a complete and precise description of the critical behavior.

*Phase diagram* - Using our SB4 method, the TMT-DMFT equations can be numerically solved to very high accuracy, allowing very precise characterization of the critical behavior. In presenting all numerical results we use units such that the bandwidth  $B = 4V = 1$ . Fig. 1a shows the resulting  $T = 0$  phase diagram at half filling, which generally [12] agrees with that of Ref. [6]. By concentrating first on the critical behavior of the QP weights  $Z_i$ , we are able to clearly and precisely distinguish the

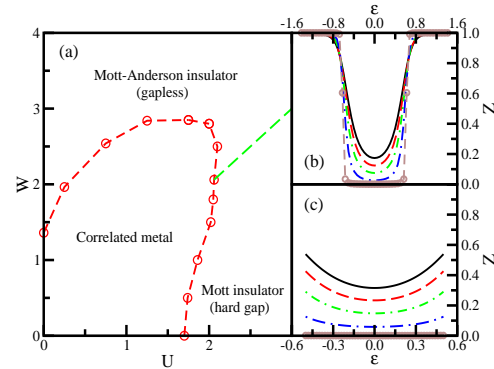


FIG. 1: (Color online) (a)  $T = 0$  phase diagram for the disordered half filled Hubbard model, obtained from the numerical SB4 solution of TMT-DMFT. Panels (b) and (c) show the evolution of the quasi-particle weight  $Z(\varepsilon_i)$  in the critical region. Behavior at (b) the Mott-Anderson transition ( $W > U$ ) is illustrated by increasing disorder  $W = 2.5, 2.6, 2.7, 2.8, 2.83$  (from the black curve to the brown one), for fixed  $U = 1.25$ ; and at (c) the Mott-like transition ( $W < U$ ) by increasing the interaction  $U = 1.5, 1.6, 1.7, 1.8$  and  $1.86$ , at fixed disorder  $W = 1.0$ .

metal from the insulator. We find that at least some of the  $Z_i$  vanish all along the phase boundary. By taking a closer look, however, we can distinguish two types of critical behavior, as follows.

*Mott-Anderson vs. Mott-like transition* - For sufficiently strong disorder ( $W > U$ ), the Mott-Anderson transition proves qualitatively different than the clean Mott transition, as seen by examining the critical behavior of the QP weights  $Z_i = Z(\varepsilon_i)$  (Fig. 1b). Here  $Z_i \rightarrow 0$  only for  $0 < |\varepsilon_i| < U/2$ , indicating that only a *fraction* of the electrons turn into localized magnetic moments. The rest show  $Z_i \rightarrow 1$  and undergo Anderson localization (see below). Physically, this regime corresponds to a spatially inhomogeneous system, with Mott fluid droplets interlaced with regions containing Anderson-localized quasi-particles. In contrast, for weaker disorder ( $W < U$ ) the transition retains the conventional Mott character. In this regime  $Z_i \rightarrow 0$  on all sites (Fig. 1c), corresponding to Mott localization of all electrons.

*Wavefunction localization* - To more precisely characterize the spatial fluctuations of the quasiparticle wavefunctions, we compare the behavior of the typical ( $\rho_{typ}$ ) and the average ( $\rho_{av}$ ) LDOS. The approach to the Mott-Anderson transition ( $W > U$ ) is illustrated by increasing disorder  $W$  for fixed  $U = 1.25$  (Fig. 2 - top panels). Only those states within a narrow energy range ( $\omega < t$ , see also Fig. 4) around the band center (the Fermi energy) remain spatially delocalized ( $\rho_{typ} \sim \rho_{av}$ ), due to strong disorder screening [7, 10] within the Mott fluid (sites showing  $Z_i \rightarrow 0$  at the transition). The electronic states away from the band center (i.e. in the band tails)

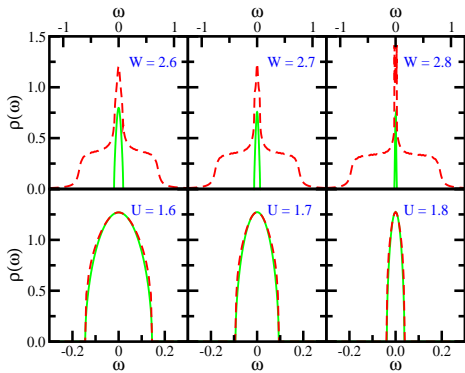


FIG. 2: (Color online) Frequency dependence of  $\rho_{typ}$  (full line) and  $\rho_{av}$  (dashed line) in the critical region. Results in top panels illustrate the approach to the Mott-Anderson transition ( $W > U$ ) at  $U = 1.25$ ; the bottom panels correspond to the Mott-like transition ( $W < U$ ) at  $W = 1.0$ .

quickly get Anderson-localized, displaying large spatial fluctuations of the wavefunction amplitudes [5] and having  $\rho_{typ} \ll \rho_{av}$ .

The spectral weight of the delocalized states (states in the range  $\omega < t$ ) decreases with disorder and vanishes at the transition, indicating the Mott localization of this fraction of electrons. At this critical point, the crossover scale  $t$  also vanishes. In contrast, the *height*  $\rho_{typ}(0)$  remains finite at the transition, albeit at a reduced  $W$ -dependent value, as compared to the clean limit. More precise evolution of  $\rho_{typ}(0)$  is shown in Fig. 3a, demonstrating its critical jump.

Behavior at the Mott-like transition ( $W < U$ ) is dramatically different (Fig. 2 - bottom panel). Here  $\rho_{typ} \approx \rho_{av}$  over the entire QP band, indicating the absence of Anderson localization. It proves essentially identical as that established for the disordered Hubbard model within standard DMFT [10], reflecting strong correlation-enhanced screening of disorder [7], where both  $\rho_{av}(\omega = 0)$  and  $\rho_{typ}(\omega = 0)$  approach the bare ( $W = 0$ ) value (see also Fig. 3b). Similar results were found in Ref. [6], but an explanation was not provided.

The corresponding pinning [7, 10] for  $\rho(\omega = 0, \varepsilon)$  is shown in the insets of Fig. 3, both for the Mott-Anderson and the Mott-like transition. In the Mott-Anderson case, this mechanism applies only within the Mott fluid ( $|\varepsilon| < U/2$ ), while within the Anderson fluid ( $|\varepsilon| > U/2$ ) it assumes smaller values, explaining the reduction of  $\rho_{typ}(0)$  in this case. We suggest that this spatial distribution of the DOS at the Fermi energy (each  $\varepsilon$  corresponds to a different position in the lattice) could be probed by scanning tunneling microscopy experiments.

*Analytical solution* - Within our SB4 approach, the TMT-DMFT order-parameter function  $\rho_{typ}(\omega)$  satisfies

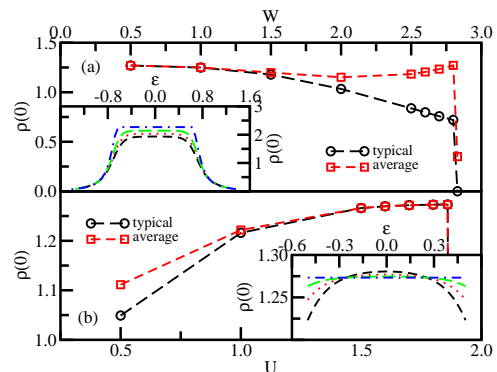


FIG. 3: (Color online) Typical and average values of  $\rho(0)$  as the metal-insulator transition is approached for (a)  $U = 1.25$  and (b)  $W = 1.0$ . The insets show  $\rho(0)$  as a function of  $\varepsilon$  for (a)  $W = 2.5, 2.6, 2.7$  and  $2.83$  (from the black curve to the blue one) and (b)  $U = 1.5, 1.6, 1.7$  and  $1.86$ .

the following self-consistency condition

$$\begin{aligned} \rho_{typ}(\omega) = \exp \int d\varepsilon P(\varepsilon) \{ & \ln[V^2 Z^2(\varepsilon) \rho_{typ}(\omega)] \\ & - \ln[(\omega - \tilde{\varepsilon}(\varepsilon) - V^2 Z(\varepsilon) \operatorname{Re} G_{typ}(\omega))^2 \\ & + (\pi V^2 Z(\varepsilon) \rho_{typ}(\omega))^2] \}. \end{aligned} \quad (3)$$

While the solution of this equation is in general difficult, it simplifies in the critical region, where the QP parameter functions  $Z(\varepsilon)$  and  $\tilde{\varepsilon}(\varepsilon)$  assume scaling forms which we carefully studied in previous work [7]. This simplification allows, in principle, to obtain a closed solution for all quantities. In particular, the crossover scale  $t$ , which defines the  $\rho_{typ}(\omega)$  mobility edge (see Fig. 4 and Ref. [7]), is determined by setting  $\rho_{typ}(\omega = t) = 0$ .

Using this approach we obtain that, in the case of Mott-like transition ( $W < U$ ), the critical behavior of all quantities reduces to that found in standard DMFT [10], including  $t \sim U_c(W) - U$  (in agreement with the numerical results of Fig. 4b), perfect screening of site randomness [7, 10], and the approach of  $\rho_{av}(\omega = 0)$  and  $\rho_{typ}(\omega = 0)$  to the clean value. The precise form of the critical behavior for the crossover scale  $t$  is more complicated for the Mott-Anderson transition ( $W > U$ ) (as confirmed by our numerical results in Fig. 4a), and this will not be discussed here.

Instead, we focus on elucidating the origin of the puzzling behavior of  $\rho_c = \rho_{typ}(\omega = 0)$ , which is known [5] to vanish linearly  $\rho_c \sim (W_c - W)$  for  $U = 0$ , but which we numerically find to display a jump (i.e. a finite value) at criticality, as soon as interactions are turned on. For  $\omega = 0$  our self-consistency condition reduces [13] to

$$\int d\varepsilon P(\varepsilon) \ln \frac{V^2 Z^2(\varepsilon)}{\tilde{\varepsilon}(\varepsilon)^2 + \pi^2 V^4 Z^2(\varepsilon) \rho_c^2} = 0, \quad (4)$$

which further simplifies as we approach the critical point. Here, the QP parameters  $Z(\varepsilon) \rightarrow 0$  and  $\tilde{\varepsilon}(\varepsilon) \sim Z^2(\varepsilon) \ll$

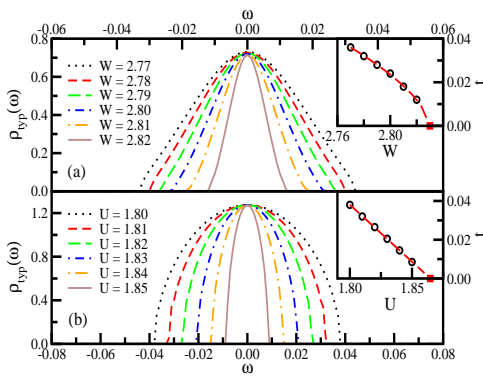


FIG. 4: (Color online) Frequency dependence of the typical DOS very close to the metal-insulator transition for (a) the Mott-Anderson transition ( $W > U$ ) at  $U = 1.25$  and (b) the Mott-like transition ( $W < U$ ) at  $W = 1.0$ . The insets show how, in both cases, the  $\rho_{typ}(\omega)$  bandwidth  $t \rightarrow 0$  at the transitions.

$Z(\varepsilon)$  for the Mott fluid ( $|\varepsilon| < U/2$ ), while  $Z(\varepsilon) \rightarrow 1$  and  $|\tilde{\varepsilon}(\varepsilon)| \rightarrow |\varepsilon - U/2|$  for the Anderson fluid ( $|\varepsilon| > U/2$ ), and we can write

$$0 = \int_0^{U/2} d\varepsilon P(\varepsilon) \ln \frac{1}{(\pi V \rho_c)^2} - \int_0^{(W-U)/2} d\varepsilon P(\varepsilon) \ln [(\varepsilon/V)^2 + (\pi V \rho_c)^2]. \quad (5)$$

This expression becomes even simpler in the  $U \ll W$  limit, giving

$$\frac{U}{W} \ln \frac{1}{\pi V \rho_c} + a - b V \rho_c + O[\rho_c^2] = 0, \quad (6)$$

where  $a(W, U) = (1 - U/W)\{1 - \ln[(W - U)/2V]\}$  and  $b = \frac{2\pi^2 V}{W}$ . This result reproduces the known result [5]  $\rho_c \sim (W_c - W)$  at  $U = 0$ , but dramatically different behavior is found as soon as  $U > 0$ . Here, a *non-analytic* (singular) contribution emerges from the Mott fluid ( $|\varepsilon| < U/2$ ), which assures that  $\rho_c$  must remain finite at the critical point, consistent with our numerical results (see Fig. 3). Note that the second term in Eq. (5), coming from the Anderson fluid ( $|\varepsilon| > U/2$ ), vanishes in the case of a Mott-like transition ( $U > W$ ), and our result reproduces the standard condition  $\pi \rho_c V = 1$  [10], which corresponds to the clean limit.

A further glimpse on how the condition  $\pi \rho_c V = 1$  is gradually violated as we cross on the Mott-Anderson side is provided by solving Eq. (5) for  $U \lesssim W$  limit, giving

$$\rho_c \approx \frac{1}{\pi V} \left[ 1 - \frac{1}{24} \left( \frac{W}{V} \right)^2 \left( 1 - \frac{U}{W} \right)^3 \right], \quad (7)$$

again consistent with our numerical solution [14].

But what is the physical origin of the jump in  $\rho_c$ ? To see it, note that the singular form of the first term

in Eq. (5) comes from the Kondo pinning [10]  $\tilde{\varepsilon}(\varepsilon) \sim Z^2(\varepsilon) \ll Z(\varepsilon)$  within the Mott fluid. This behavior reflects the particle-hole symmetry of our (geometrically averaged)  $\rho_{typ}(\omega = 0)$  bath function, which neglects site-to-site cavity fluctuations present, for example, in more accurate statDMFT theories [15]. Indeed, in absence of particle-hole symmetry, one expects [10]  $\tilde{\varepsilon}(\varepsilon) \sim Z(\varepsilon)$ , and the resulting  $\varepsilon$ -dependence should cut-off the log singularity responsible for the jump in  $\rho_c$ . This observation provides a direct path to further refine the TMT-DMFT approach, reconciling the present results with previous statDMFT findings [15]. As a next step, one should apply the TMT ideas to appropriately chosen effective models [16], in order to eliminate those features reflecting the unrealistic particle-hole symmetry built in the current theory. We emphasize that the two-fluid picture is a consequence of only a fraction of the sites showing  $Z \rightarrow 0$  and is not dependent on either particle-hole symmetry or the consequent jump in the DOS.

*Conclusions* - This Letter explores the TMT-DMFT critical region of the Mott-Anderson transition. We show how key insight can be obtained by focusing on the evolution of the local quasiparticle weights  $Z_i$  as a *second order parameter* describing tendency to Mott localization, in addition to the Anderson-like TMT order parameter  $\rho_{typ}$ . This analysis reveals the fundamental two-fluid character of the Mott-Anderson transition, consistent with the phenomenology proposed for doped semiconductors [8]. Physically, it describes spatially inhomogeneous situations, where the Fermi liquid quasiparticles are destroyed only in certain regions - the Mott droplets - but remain coherent elsewhere. Understanding the details of such “site selective” Mott transitions should be viewed as an indispensable first step in solving the long-standing problem of metal-insulator transitions in disordered correlated systems.

We thank Dieter Vollhardt for useful discussions. This work was supported by PRPq/UFMG and CNPq grant 473987/2007-4 (M.C.O.A.) and NSF grants DMR-0234215 and DMR-0542026 (V.D.), and DMR-0096462 (G.K.).

- 
- [1] N.F. Mott, *Metal-insulator Transitions* (Taylor and Francis, London, 1974).
  - [2] P.W. Anderson, Phys. Rev. **109**, 1498 (1958).
  - [3] P.A. Lee and T.V. Ramakrishnan, Rev. Mod. Phys. **57**, 287 (1985).
  - [4] A. Georges *et al.*, Rev. Mod. Phys. **68**, 13 (1996).
  - [5] V. Dobrosavljević *et al.*, Europhys. Lett. **62**, 76 (2003).
  - [6] K. Byczuk *et al.*, Phys. Rev. Lett. **94**, 056404 (2005).
  - [7] M.C.O. Aguiar *et al.*, Phys. Rev. B **73**, 115117 (2006); Physica B **403**, 1417 (2008).
  - [8] M. A. Paalanen *et al.*, Phys. Rev. Lett. **61**, 597 (1988).
  - [9] L. De Leo *et al.*, Phys. Rev. B **77**, (075107) (2008); see also: Phys. Rev. Lett. **101**, 256404 (2008); A. Koga *et al.*

- al.*, Phys. Rev. Lett. **92**, 216402 (2004); A. Camjayi *et al.*, Nature Physics **4**, 932 (2008).
- [10] D. Tanasković *et al.*, Phys. Rev. Lett. **91**, 066603 (2003).
- [11] G. Kotliar and A.E. Ruckenstein, Phys. Rev. Lett. **57**, 1362 (1986).
- [12] We do not discuss the coexistence region found in Ref. [6], because we focus on criticality within the metallic phase. We do not find any “crossover” regime such as reported in Ref. [6], the existence of which seems inconsistent with the generally sharp distinction between a metal and an insulator at  $T = 0$ .
- [13] For our model  $\text{Re}G_{typ}(0) = 0$  by particle-hole symmetry.
- [14] In this respect, our results differ from those in Ref. [6], where  $\rho_c$  is shown to vanish for large  $U$ . This seems to occur within what the authors call the “crossover” regime, which is not present in our phase diagram (see Ref. [12]).
- [15] V. Dobrosavljević and G. Kotliar, Phys. Rev. Lett. **78**, 3943 (1997).
- [16] D. Tanasković *et al.*, Phys. Rev. B **70**, 205108 (2004).